Low-Loss, Low-Back-Reflection Fusion Splicing Of Large-Mode-Area Fibers With Nested Hollow-Core Antiresonant Fibers For All-fiber High-Power, Single-Frequency Fiber Laser Transmission

Yu Wen, Xin Zhang, Weihua Song, Jingyuan Yao, Mengyao Cui, Qian Zhang, Shuai Gu, and Pu Wang

***Abstract*—The all-fiber integration of hollow-core fibers (HCF) with high-power fiber laser systems remains a significant technical challenge, hindering their scale-up in laser applications. In this study, we demonstrate a low-loss, low-back-reflection, high-power fusion between a nested hollow-core antiresonant fiber (Nested HC-ARF) and a large-mode-area fiber (LMA) using fiber up-taper and angle splicing technology. A minimum fusion loss of 0.29 dB was achieved at a 0° angle when the two types of fibers were mode-field matched. Based on this, we investigated the relationship between back-reflection suppression and fusion loss for Nested HC-ARF and LMA, achieving a balance between them. The best performance was achieved at an angle-cleave of approximately 2°, where the back reflection was suppressed to below -30 dB, and the fusion splice loss was 0.44 dB. Finally, utilizing this fusion splicing technology, we have, for the first time, achieved all-fiber single-frequency pulsed fiber laser transmission using Nested HCFs, with a maximum input power of 62.92 W and a fiber splice point temperature maintained at 28 °C over a 20 m length of Nested HC-ARF. The time-frequency characteristics of single-frequency pulsed lasers remain well-preserved before and after transmission. Our approach enables efficient all-fiber integration between HCFs and high-power fiber laser systems, facilitating HCFs for a wide range of applications in laser processing, and gas sensing.**

***Index Terms*—Optical fiber splicing, hollow-core fiber, angle-cleaved fiber, high-power laser transmission.**

I. INTRODUCTION

Hollow core fibers (HCFs) provide nearly free-space propagation conditions for light waves by confining light within an air core with a low refractive index, thereby enabling flexible transmission. This approach significantly overcomes the limitations of conventional single-mode fibers (SMFs) in terms of dispersion, nonlinearity, and the damage threshold. It offers new avenues for development in application fields such as fiber laser transmission and gas laser generation, fiber-optic communications, and fiber sensing [1-3]. In high-power fiber laser transmission, traditional solid-core fibers introduce aberrations into the transmitted laser light due to nonlinear effects and dispersion. Conversely, HCFs, which guide light through an air core, exhibit low nonlinearity and high damage thresholds [7-9], offering a viable solution for high-power laser transmission applications. Recent research has achieved several milestones in HCFs, including 3 kW high-power continuous lasers [10], a 30 mJ single-pulse energy [11], a 20 GW peak power [12], and 1-km long-distance power transmission in the kilowatt range [13]. These results underscore the significant potential of HCFs for high-power laser transmission applications. In addition, in the field of mid-infrared fiber lasers, current rare-earth-doped fiber lasers have difficulty generating laser outputs greater than 3 μm and exhibit low power levels. Instead, by utilizing gases within HCFs and leveraging their wide range of emission wavelengths, mid-infrared laser outputs featuring a broad wavelength coverage, a high power, and a superior beam quality can be realized. Mid-infrared laser outputs of 21.8 W [5] and 6.6 W [6] at 3.1 μm and 4.3 μm, respectively, have been reported.

However, in the application fields described above, the approach to HCF incorporation into fiber laser systems is usually established by free-space coupling techniques using a variety of optical components (including focus lenses and reflective mirrors). Although this method can handle high-power transmission, on the one hand, its overall device is more complex, exhibits relatively poor stability, and is susceptible to environmental disturbances. On the other hand, the thermal effect produced by the coupling lens during the transmission of a high-power laser is prone to cause a focus shift, thus affecting the transmission efficiency[10], which is a considerable obstacle to miniaturization and integration.In summary, how to solve the problem of efficient all-fiber connection between HCFs and high-power fiber laser systems remains to be explored.

Interconnections between HCFs and solid-core fibers need to address relatively large mode-field diameters (MFDs) differences and about 3.4% Fresnel reflections [14]. Most of the connectivity work reported to date has focused on a low

This work was supported in part by the National Natural Science Foundation of China under Grant 62035002, Grant 62305014, Grant U2241225, and in part by the China Postdoctoral Science Foundation under Grant 2023M730139. (Corresponding authors: Xin Zhang, Pu Wang.)

Yu Wen, Xin Zhang, Weihua Song, Jingyuan Yao, Mengyao Cui, Qian Zhang, Shuai Gu, and Pu Wang are with the Institute of Laser Engineering, Physics and Optoelectronic Engineering, Beijing University of Technology, Beijing 100124, China (email: wenyu09262022@163.com, zhangxin940425@bjut.edu.cn, 1148368737@qq.com, yaojy@emails.bjut.edu.cn, 3473659741@qq.com, zhangqian09236@bjut.edu.cn, shuaigu@bjut.edu.cn, wangpuemail@bjut.edu.cn).

Color versions of one or more figures in this article are available at https://doi.org/xxxxxxxx

connectivity loss between SMFs and HCFs. For example, an insertion loss of 0.88 dB for SMF/HCF/SMF fiber links has been achieved via fiber up-tapering and a thermally expanded core (TEC) for SMFs [15]. Additionally, a coupling loss of 0.079 dB between SMF-28 and HCF can be attained by bridging a gradual refractive index multimode fiber with an HCFs, which is then coated with an anti-reflection coating [14]. These advancements primarily pertain to fusion splicing or joining of standard SMFs with HCFs, mainly for fiber-optic communications with relatively low transmission power. However, in the field of high-power fiber lasers, LMAs (core diameters between 20 μm and 30 μm) are widely used because of their greater power scalability and higher nonlinearity thresholds. But less research has been done on efficient connection technologies between these LMAs and HCFs. Furthermore, the interaction between an HCF and an LMA generates back-reflected light due to differences in transmission media, which, when amplified in the active optical fiber, may cause the output power to decline or may even cause system damage [16]. Currently, the main methods for back reflection suppression include anti-reflection coatings and fiber angle-cleaved. Anti-reflection coatings have been shown to reduce back reflection in SMF-28/HCF/SMF-28 fiber links to levels between -28 dB [17] and -35 dB [18]. However, these coatings have a limited tolerance, particularly under high-power laser conditions, which can lead to localized splicing and irreversible damage. The technique of angle-cleave and fusion splice of fibers employing gradually graded index multimode fibers results in a connection loss of 1.25 dB and back reflection levels below -40 dB [19]. Angled fusion splicing significantly reduces back reflection, but this method comes at the expense of the fusion splicing efficiency,when the fusion splicing efficiency is low, the cumulative thermal effect generated at the fiber connection point during laser transmission can lead to fiber damage. Consequently, in applications such as high-power fiber laser transmission and gas laser generation, the development of HCF all-fiber connection technology that ensures a high connection efficiency and suppresses back reflection remains a challenge to be resolved at this time.

In this study, we demonstrated a low-loss, low-back-reflection, high-power fusion technique between an Nested HC-ARF and an LMA. A fusion splice loss of 0.29 dB at an angle of 0° is achieved via the up-tapering technique for the LMA. We investigated the relationship between back reflection suppression (which improves with increasing cutting angle [20]) and splice loss (which worsens with increasing cutting angle) and achieved a balance between them. Experiments show that the best performance is achieved at a cutting angle of approximately 2°, at which the back reflection is suppressed to below -30 dB, compared with -14.9 ±0.2 dB for a flat-angle splice, and the fusion loss is 0.44 dB, which is an increase of 0.15 dB compared with the flat-angle fusion loss. Finally, we demonstrated for the first time the all-fiber transmission of a single-frequency pulsed laser inside the Nested HC-ARF based on the above fusion technology. Where the highest input power is 62.92 W, the Nested HCF transmission length is 20 m, and the measured splicing point temperature was about 28℃. The laser characteristics before and after transmission is well maintained, demonstrating the all-fiber integration, distortion-free, and flexible transmission of high-power single-frequency pulsed lasers based on HCF.

II. Simulation and Experimentation of an HCF and an LMA

A, Principle and analysis

The commercial passive fiber CJGDF-LMA-25/300 purchased from Wuhan Changjin Photonics Technology Co, with a core diameter of 25 μm, a cladding diameter of 300 μm, an operating wavelength range of 1530 nm-1800 nm, and a numerical aperture(NA) of 0.085, is utilized in the experiments. At 1535 nm, the transmission loss and mode-field diameter (MFD) of the fiber are measured as 0.049 dB/m and 23.2 μm, respectively. Fig.1(a) presents the cross-sectional structure of the Nested HC-ARF, which was imaged via scanning electron microscopy (SEM). This fiber comprises six uncontacted nested tubes with an inner diameter (ID) of 39 μm, a cladding diameter of 230 μm. The fiber has a MFD of 29.2 μm, an NA of 0.035, and a transmission loss of 0.85 dB/km at 1535 nm. Fig.1(b) and (c) illustrate the near-field beam profiles of the Nested HC-ARF and LMA, respectively, captured by a charge-coupled device (CCD) camera employed for beam profile observation. An analysis reveals that the beam profile of the Nested HC-ARF is significantly larger than that of the LMA, with the beam profile situated in the outermost energy-weak region of the fiber mode field exhibiting a distinct hexagonal feature.

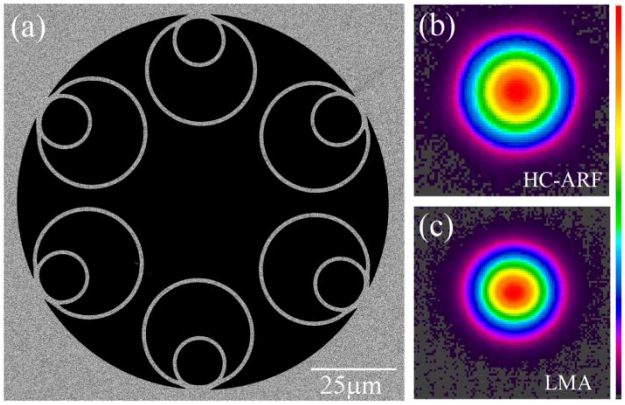

Fig.1. (a) SEM image of 6-tube Nested HC-ARF. (b-c) Near-field beam profiles (b) the Nested HC-ARF (c) the LMA

A wide range of factors influence fiber optic loss. Depending on whether the source of loss is related to the characteristics of the fiber itself, connection loss can be categorized into intrinsic joint loss and nonintrinsic joint loss. This discussion primarily focuses on intrinsic joint loss. Intrinsic joint loss primarily arises from mode-field mismatch between Nested HC-ARFs and solid-core fibers, as well as Fresnel reflection resulting from differences in the light-conducting medium [21]. The predominant source of loss is attributed to the mode-field mismatch; to more precisely describe optical coupling loss, in the absence of any misalignment of connection points, we can introduce a

mathematical expression to represent it [22]:

$$\alpha = 1 - \left| \frac{2\langle E_t | H_i \rangle \langle E_i | H_t \rangle}{\left(\langle E_t | H_i \rangle + \langle E_i | H_t \rangle \right)} \right|^2 \quad (1)$$

where Ei and Hi are the normalized electric and magnetic field vectors of the LMA fundamental mode, respectively, and Et and Ht are the corresponding electric and magnetic fields of the HCF:

$$\left\langle E_{t(i)} \middle| H_{t(i)} \right\rangle = \frac{1}{2} \mathrm{Re} \left(\int dA \left(E_{t(i)} \times H_{t(i)}^{*} \right) \cdot \hat{z} \right) = 1 \quad (2)$$

As indicated in the above equation, when the mode field distributions of the two fibers perfectly match—specifically, when the MFDs and mode shapes are identical—the overlap integral in the equation becomes 1, resulting in zero coupling loss. Consequently, to minimize the fusion splice loss between the HCF and the LMA with a large mode field, addressing the issue of mode-field mismatch as a priority is imperative.

We initially simulated and analyzed the modal distributions of the HCF and the LMA via the full vector finite element mode solver in COMSOL, as depicted in Fig.2(a). By accurately modeling the two fibers, the MFDs of the LMA and HCF at 1535 nm were calculated to be 23.2 μm and 29.2 μm, respectively. We subsequently measured the variation in the MFDs with the diameter of the LMA cladding during the fiber up-tapering, alongside the corresponding coupling loss for the HCF. As illustrated in Fig.2(b), the coupling loss resulting from the mode-field mismatch between the untreated LMA and HCF is 0.74 dB, equivalent to a coupling efficiency of 84.3%. The cladding diameter of the tapered fiber scales proportionally with the core diameter, and its MFD ranges between 23.0 μm and 32.0 μm. The results indicate that the coupling loss between the two fiber types initially decreases before subsequently increasing. The minimum coupling loss of 0.083 dB is achieved under mode-field matching conditions when the cladding diameter of the LMA is 368.2 μm, which coincides with an MFD of 29.2 μm. This finding offers theoretical guidance for subsequent studies.

B, Tapering and LMA-Nested HC-ARF splicing

We demonstrated mode-field matching between Nested HC-ARFs and large-core-diameter solid-core fibers through the use of fiber up-tapering, which is a fiber processing technique in which both the core and cladding are enlarged by nearly the same ratio while maintaining the original refractive index of the fiber [23]. Precise alignment of the fiber and control of compressive stress are crucial to minimize the additional losses introduced during the up-tapering process. We employed FPS 1.8b software to configure the parameters of the Fujikura FSM-100P+ fusion splicer for up-tapering of LMAs. The fiber was stripped, secured between two precisely aligned fixtures of the fusion splicer, and then subjected to discharge and splicing, followed by inward advancement from both ends under software control. The propulsion speed was set at 1 mm/s, the discharge power in the waist zone was 333 units, and the total duration of the up-tapering process was 25 seconds. The desired waist zone diameter was achieved by adjusting the discharge power, initial fiber diameter, and propulsion speed. By controlling these parameters, we could expand the fiber to the desired cladding diameter, with the dopant ion diffusion effect being negligible due to the brief duration of the up-tapering process [24]. This method enabled us to produce an up-taper LMA with a nearly ideal appearance and shape, featuring a taper and transition region total length of approximately 2.5 mm, which is significantly longer than the beat length between higher-order modes of the fiber (<1 mm), where the excited higher-order modes carry considerably less energy than the fundamental mode [18]. The MFD of the fiber was measured using a telescope system composed of two convex lenses with focal lengths of 40 mm and 200 mm, respectively. Following collimation and magnification of the beam, the beam waist values in the image plane were scanned and measured using a Thorlabs BP109-IR1 beam quality analyzer. To ensure the accuracy of the measurement system, an SMF-28 fiber was utilized for calibration. Fig. 3(a) shows the variation in the fiber MFD with the cladding diameter post-pulling, indicating that the beam shape remains unchanged after the up-taper treatment. The actual measurements of the core and cladding reveal almost identical enlargement ratios, which is consistent with the simulation results.

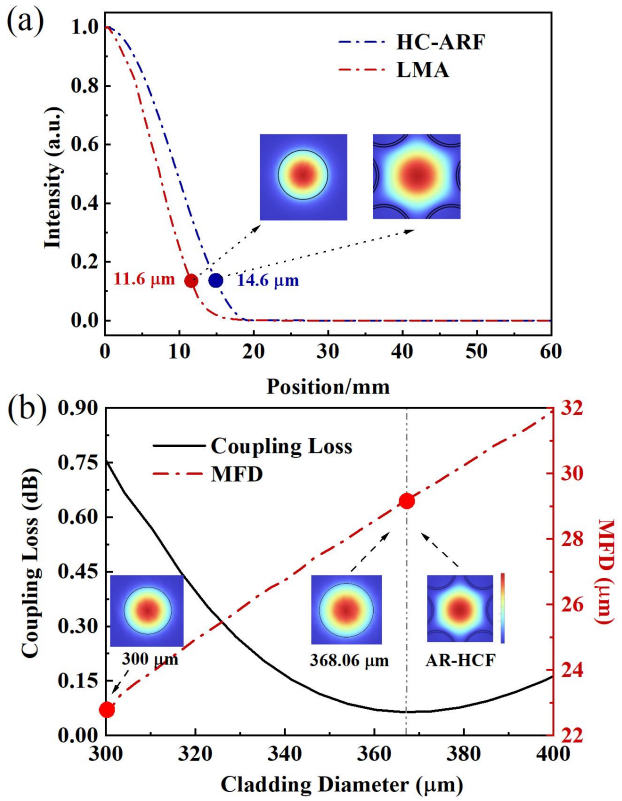

Fig. 2. (a) Normalized image of the light intensity decay with increasing beam radius. (b) Variation of MFD with up-tapered LMA fiber diameter (red dashed line); corresponding coupling loss when the HCF is connected (black solid line).

The thickness and capillary shape of the Nested HC-ARF directly affects its transmission characteristics, and

conventional fusion welding procedures often result in the collapse and deformation of the capillary tube, which greatly increases fusion losses. To minimize the collapse of the microstructure in the Nested HC-ARF during the fusion splicing process and optimize the strength at the fusion point, we optimized the parameters of the Fujikura FSM-100P+ fusion splicer via the control variable method. Parameters such as the discharge power, discharge time, and overlap were adjusted. A up-tapered LMA with a discharge power of 55 units, a discharge time of 8000 ms, and a 10 μm overlap was employed for fusion splicing with an Nested HC-ARF. The over-offset discharge technique was utilized to shift the Nested HC-ARF by 50 μm from the electrodes, ensuring that there was no significant deformation of the cladding pores in the fusion-spliced Nested HC-ARF and achieving a fusion point with a high mechanical strength. The splicing losses of the up-tapered fiber to Nested HC-ARFs with different cladding diameters were measured, as shown in Fig.3(b). single-frequency laser with a wavelength of 1535 nm, a bandwidth of 0.0802 nm, and a power of 1 W served as the light source. The output power (P_{in}) of a single LMA was measured via a photosensitive power meter (Thorlabs-S146C). The LMA was then cut in the middle, and LMAs with various pulled-taper sizes were fusion spliced with Nested HC-ARFs. The output power Pout at the Nested HC-ARF end was obtained for different pulled-taper sizes, with the results calculated through $\text{loss} = -10\log\frac{P_{out}}{P_{in}}$. The initial length of the Nested HC-ARF used was 20 m. The measured loss trend closely follows the simulation results. The lowest achievable splice loss of the LMA-Nested HC-ARF is 0.27 dB, and the average fusion loss is 0.29±0.02 dB when the cladding size is tapered to approximately 360 μm. These results confirm effective mode-field matching between the Nested HC-ARF and LMA, with further reductions in fusion loss expected through decreased Fresnel reflection [14]. Additionally, there is a slight deviation between the experimental results and simulations for the lowest fusion splice loss corresponding to a cladding diameter of 368.2 μm. This discrepancy is due to the MFD obtained from the up-taper fiber being slightly larger in actual experiments than in simulations. The MFDs of the two 360.0 μm and 368.2 μm tapered fibers are 29.3±0.4 μm and 29.5±0.3 μm, respectively, with the MFDs of the LMAs being closer to the Nested HC-ARF MFD when the taper is drawn to 360.0 μm. The inset of Fig.3(b) shows a microscopic cross-section of the fusion point obtained using the optimal fusion splicing parameters, revealing a stable fusion point and no significant deformation of the Nested HC-ARF capillary. This method is expected to be suitable for matching different types of specialty fibers. Although our up-taper process may not achieve perfect cladding size matching for all specialty fibers, it significantly reduces the mode-field mismatch and thus mitigates loss.

In addition to the interfiber mode-field mismatch problem, Fresnel reflection at the interface of the Nested HC-ARF-to-solid-core fiber fusion in high-power transmission systems is also a concern, which may cause damage to the laser system. Therefore, the Fresnel reflection at the interface of Nested HC-ARFs and solid-core fibers in such applications needs to be strictly suppressed. Angled cutting of optical fibers is usually an effective method. However, the fusion splice loss between the Nested HC-ARF and the LMA directly affects

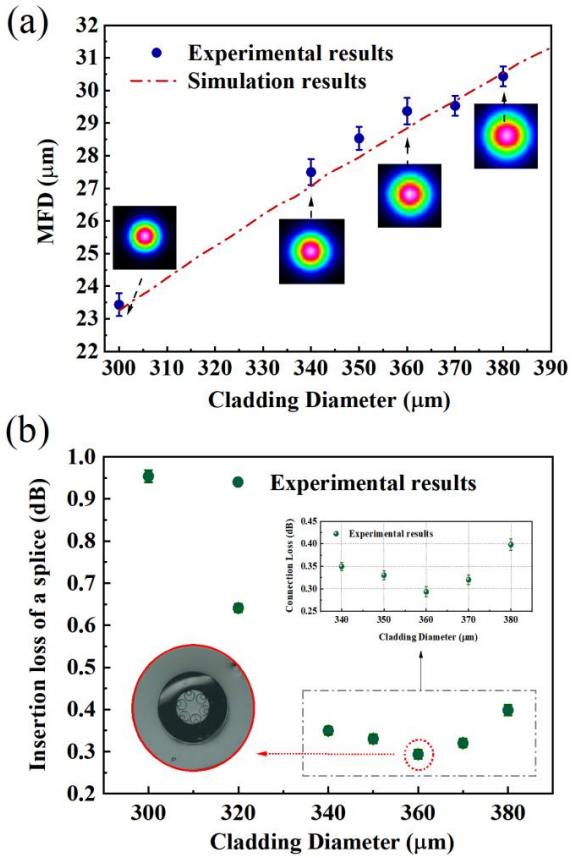

Fig. 3. (a) Images of the fiber MFD with varying cladding diameter after tapering. (b) Measured fusion splice loss trend with the cladding diameter, Inset: results of multiple interconnections from 0-2°.

heat accumulation at the fusion point, and an increased loss at the fusion splice causes the temperature at the fusion point to rise, causing thermal damage to the fiber. Therefore, the experiments require a trade-off between back-reflection suppression and a high joining efficiency.

C, Angled cleavage and splicing

Experiments were conducted using a large-core-diameter cutter (Vytran, LDC-400) to achieve the desired fiber cutting angle. The fiber was placed in a fiber fusion splicer equipped with a video camera and software for measuring the face angle, resulting in an angle accuracy of approximately 0.2°. The same single-frequency fiber laser as that utilized in the previous experiments served as the light source, and the back reflection of the LMA was measured at various angles by incorporating a circulator into the laser pigtail. A flat-cleaved LMA was calibrated and subsequently cut to different angles; a photosensitive power meter (Thorlabs-S146C) was employed to measure the power of both the two-port LMA and the three-port circulator, thereby obtaining back-reflection

values. Fig. 4(b) presents the back-reflection values of the LMA at different angles. As shown in Fig.4(b), the back-reflection level decreases with increasing fiber cutting angle. This phenomenon occurs because, as the fiber cutting angle increases, the back-reflected light generated at the interface between the air and the fiber does not return to the core in the same manner as it does at a flat angle; rather, it is refracted out of the fiber as the angle of the fiber end face increases. A 20 m Nested HC-ARF was subsequently connected to the laser system via the aforementioned angular fusion joining method, and the output power (P_{out}) at the Nested HC-ARF end was measured. Experimental samples of LMA-Nested HC-ARF fibers with various cutting angles were prepared. Fig.4(c) shows the variation in the fusion splice loss with the cutting angle, with the inset displaying the results of five interconnections for angles ranging from 0° to 2°, with the measurement error characterized through the standard deviation. The fusion loss progressively increases with increasing cutting angle. With our angled splicing technique, the splice loss can be kept below 1 dB over a 2° range, with a splice loss of 0.37 dB and a back reflection of -22.6±0.1 dB for 1° spliced fibers, and a splice loss of 0.44 dB and a back reflection of -30.4±0.2 dB for 2° samples, with the splice loss reaching 4.02 dB at an angle of 6.6°. Thus, a trade-off exists between back-reflection suppression and splice loss. Notably, the angle splicing of Nested HC-ARF to LMA method achieves a back-reflection reduction exceeding 15 dB at 2° compared with flat fusion joining while only increasing the joining loss by 0.15 dB, ensuring efficient transmission and mitigating the risk of damage to high-power laser sources.

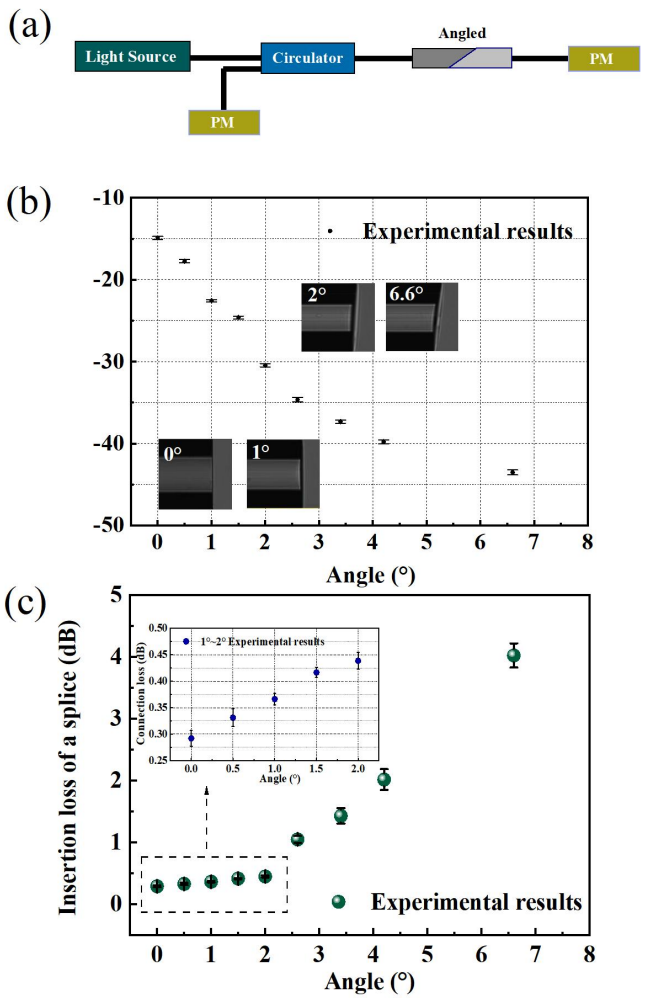

Fig. 4. (a) Diagram of the experimental setup for measuring the back reflection and fusion splice loss. (b) Variation in the back reflection with the angle, the inset shows side images of the fibers with different angles. (c) Splice loss for different angles.

III. High-power single-frequency fiber laser transmission validation

To verify the feasibility of the LMA and Nested HC-ARF joining method in high-power laser systems, we applied the aforementioned 2° angle fusion joining technique to a high-power laser system. The high-power laser employed in the experiments was a laboratory-developed 1.5 μm single-frequency nanosecond fiber laser, as illustrated in Fig.5(a). This system comprises a distributed feedback single-frequency laser (DFB-SFL) and a three-stage erbium-doped fiber amplifier. The output laser had a central wavelength of 1535.39 nm, a signal-to-noise ratio exceeding 50 dB, a free spectral range of 10 GHz, and a corresponding linewidth of approximately 145 MHz. The output pigtail of the source was a CJGDF-LMA-25/300.

The pigtail was angled-splice to a 20 m-long Nested HC-ARF, which had a bending diameter of 60 cm. A power meter (Gentec-e) was employed to measure the optical power before and after fusion splicing, and the transmission efficiency was calculated accordingly. In this experiment, the splice point was secured to a water-cooled plate with a groove that was approximately 1 mm wide. Fig.5(b) shows the variation in the output power and beam quality at the Nested HC-ARF tail end with the input power. The sample demonstrates a high transmission efficiency at an input power below 8.86 W, where the transmission efficiency is 90.4%. The laser quality and the quality of the beam after passing through the Nested HC-ARF are characterized by M^2_x=1.05 and M^2_y=1.10 and by M^2_x=1.04 and M^2_y=1.09, respectively (measured via Thorlabs BP209), indicating that the beam output from the laser, as wellas after traversal through the Nested HC-ARF, predominantly transmits in the fundamental mode, as depicted in Fig.5(c). When the output power of the Nested HC-ARF is increased from 8.86 W to 28.92 W, the overall transmission efficiency decreases from 90.5% to 81.3%. This decline is attributed primarily to the continuous deterioration of the quality of the output beam, which results from the gradual increase in the higher-order mode content during the power-boosting process (M^2_x=1.29 and M^2_y=1.34 at 28.92 W) .

The quality of the output beam of the Nested HC-ARF remains below 1.1 because of the implementation of a 6-tube nested Nested HC-ARF designed for effective single-mode transmission. Within the Nested HC-ARF, light is guided in the air core via ultrathin negative curvature walls ranging from hundreds of nanometers to a few micrometers, allowing

efficient filtering of higher-order modes (HOMs) in the core through coupling with cladding modes when the phase-matching condition is satisfied. When the output power of the Nested HC-ARF is increased from 28.92 W to 36.83 W, the transmission efficiency stabilizes at approximately 81%, and the beam quality at this stage stabilizes at approximately 1.3.

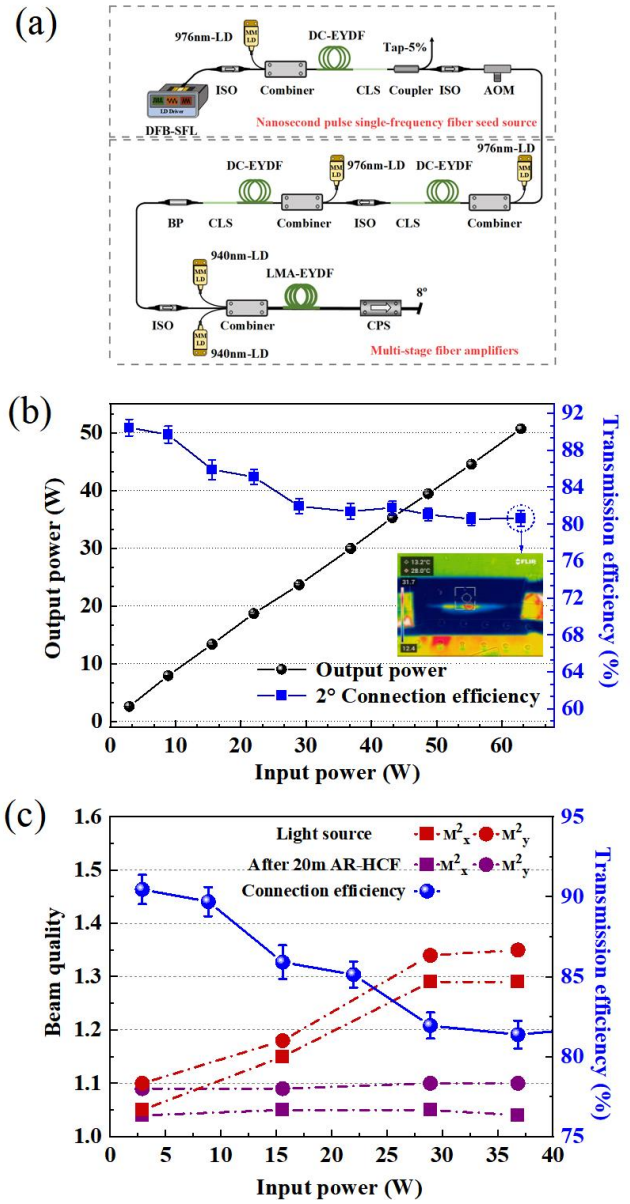

Fig. 5. (a) Image of the laser source unit. (b) Variation in the output power and fusion efficiency with the input power, the inset shows the temperature of the fusion point at the highest output power. (c) Variation in the beam quality and fusion efficiency with the input power before and after fusion welding.

Owing to laboratory constraints and the safety of the measurement instruments, we only measured the beam quality with an input power of 36.83 W. The beam quality of the laser input matches that of the output, which subsequently affects the overall transmission efficiency. Limited by the input source laser power, the maximum input power of 62.92 W results in an output power of 50.73 W after splicing of the Nested HC-ARF, achieving a fusion efficiency of 81.3%. The temperature of the Nested HC-ARF coating after initial stripping and slicing was monitored via a thermal imaging camera, as shown in the inset of Fig.5(c). At the highest input power of 62.92 W, the maximum temperature at the splice point is 28°C, which is clearly below the failure temperature of the fiber coating (~100°C), suggesting that the fusion bonding technology can also handle higher temperature gradients and has a higher power tolerance potential.

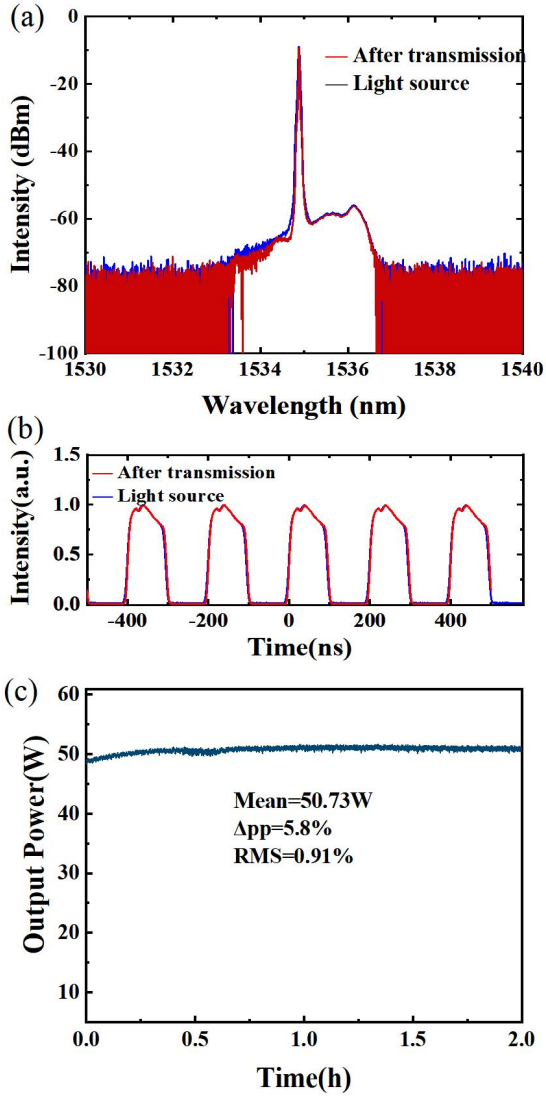

Fig. 6. (a) Normalized optical spectra of laser pulses before and after transmission in the 20 mlong HC-ARF when the incident pulse energy is 14 μJ. (b) Pulsed width before and after transmission through the HC-ARF. (c) Long stability test for output powers. Here RMS denotes the root mean square deviation.

In addition, the spectra and pulse widths before and after laser transmission were experimentally measured to investigate whether fusion splicing of the Nested HC-ARF affects the characteristics of the input single-frequency nanosecond laser. An optical spectrometer (YOKOGAWA-AQ6370D) was used to scan the entire spectral region, as shown in Fig.6(a). The measured output spectrum of the 20 m Nested HC-ARF is consistent with the incident spectrum. The measured temporal distribution of the transmission pulse when

the incident pulse energy is 14 μJ is depicted in Fig.6(b), demonstrating the average transmission pulse width over the 20 m Nested HC-ARF. For these measurements, InGaAs (Thorlabs, DET08CFC/M) and a high-speed oscilloscope (DSOX6002A) were used. The half-maximum at full-width of the Gaussian fit to the pulse profile was calculated as the pulse width. The laser pulse width remains at 93 ns through the 20-meter Nested HC-ARF, which is essentially unchanged from the pulse width of the incident laser. This series of characterizations of the laser transmission properties indicates that the all-fiber fusion and energy transfer technique employed can achieve distortion-free transmission of high-power single-frequency pulsed lasers. Additionally, at an output power of 50.73 W, we performed a two-hour stability test on the splice point, with the experimental results presented in Fig. 6(c). The experimental results show that the peak power fluctuation(Δpp) is 5.8%, the root mean square error(RMS) is 0.91%, and the output laser is basically stable, which verifies the stability of this Nested HC-ARF fusion splicing technology.

IV. Conclusion

In summary,we demonstrate a low-loss, low-back-reflection, high-power fusion between an Nested HC-ARF and an LMA. Initially, fiber up-taper is employed to achieve mode-field matching between the LMA and Nested HC-ARF, ensuring a low-loss fusion. The additional loss attributed to the fiber up-taper process is less than 0.01 dB. The further loss attributable to the fiber up-taper process remains below 0.01 dB, while samples of LMA-HCF fiber fusion splices fabricated using this method exhibit a minimum loss of 0.27 dB. Subsequently, back-reflection arising from differences in the refractive index of the fiber cores is minimized through angle-cleave techniques. By balancing the back-reflection and fusion loss, low back-reflected light is ensured while maintaining high fusion efficiency. The angled fusion splicing technology demonstrates a fusion loss of 0.44 dB at an angle of 2 ° and yields a back reflection of less than -30 dB. Ultimately, a stable and efficient LMA-HCF laser output was achieved by employing a laboratory-made high-power single-frequency pulsed fiber laser as the input source. When the input power exceeds 60 W, the single pulse energy is 14 μJ, and the fusion point temperature remains below 28°C. By measuring the spectra and pulse widths before and after transmission, the fused and spliced single-frequency nanosecond laser pulses maintain good single-frequency and pulse characteristics during transmission through the 20-meter-long Nested HC-ARF. We experiment demonstrates integrated transmission of high-power lasers via all-fiber technology based on an Nested HC-ARF, confirming the viability of using Nested HC-ARFs for high-power fiber laser transmission. Moreover, by fusion splicing solid-core fibers with HCFs, we provide a potential pathway to enhance the performance of high-power continuous and ultrafast pulsed fiber lasers by leveraging the modal characteristics of HCFs. In addition, our application of this Nested HC-ARF fusion splicing technique to continuous lasers is still efficient and feasible. Our fusion splice technology makes HCFs promising for large-scale applications in scientific and industrial fields. In the future, we will perform a systematic theoretical analysis and develop relevant models for the angular connection values of solid-core fiber and hollow-core fibers with varying core sizes and mode content, which will yield more comprehensive theoretical insights for this type of splicing work. In the splicing process, we aim to enhance the fusion strength by employing the Tack Sweep Pulse (TSP) [26] fusion method. Furthermore, in future research, we intend to achieve improved operational stability and enhance the capacity to withstand higher transmission power through the utilization of the HCF cable.

References

[1] R. F. Cregan, B. J. Mangan, J. C. Knight, et al. Single-mode photonic band gap guidance of light in air [J]. Science, 1999, 285:1537-1539.
[2] M. Komanec, D. Dousek, D. Suslov, et al. Hollow-Core Optical Fibers[J]. Radioengineering, 2020, 29(3): 417–430.
[3] C. Wei, R. J. Weiblen, C. R. Menyuk, et al. Negative curvature fibers[J]. Advances in Optics and Photonics, 2017, 9(3): 504.
[4] W. Huang, Z. Zhou, Y. Cui, et al. “4.5w mid-infrared light source based on acetylene-filled hollow-core fibers,” Opt. Laser Technol. 151, 108090 (2022).
[5] Song, W., Yao, J., Zhang, X., Zhang, Q., Hou, Y., Wu, J., & Wang, P. (2024). 4.3 μm high-power amplified spontaneous emission fiber source based on CO2-filled nested hollow-core anti-resonant fiber. Optics express, 32 8, 14532-14540 .
[6] W. Song, X. Zhang, Q. Zhang, Y. Hou, and P. Wang, "21.8 W acetylene-filled hollow-core anti-resonant fiberamplified spontaneous emission source at 3.1 μm," Opt. Lett. 49, 3636-3639 (2024).
[7] Poletti F. Nested antiresonant nodeless hollow core fiber[J]. Optics Express, 2014, 22(20): 23807-23828.
[8] Shephard J D, Couny F, St J Russell P, et al. Improved hollowcore photonic crystal fiber design for delivery of nanosecond pulses in laser micromachining applications[J]. Applied Optics, 2005, 44 (21): 4582-4588.
[9] Roberts P J, Couny F, Birks T A, et al. Achieving low loss and low nonlinearity in hollow core photonic crystal fibers[C] Conference on Lasers and Electro-Optics, May 22-27, 2005, Baltimore, MD, USA. New York: IEEE Press, 2005: 1240-1242.
[10]J. Yao et al., "High-Efficiency Distortion-Free Delivery of 3 kW Continuous-Wave Laser Using Low-Loss Multi-Mode Nested Hollow-Core Anti-Resonant Fiber," in Journal of Lightwave Technology, vol. 42, no. 16, pp. 5710-5716, 15 Aug.15, 2024
[11]Dumitrache C, Rath J, Yalin A P. High power spark deliveryystem using hollow core kagome lattice fibers[J]. Materials, 2014, 7(8): 5700-5710.
[12]Lekosiotis A, Belli F, Brahms C, et al. On-target delivery of intense ultrafast laser pulses through hollow-core anti-resonant fibers[J]. Optics Express, 2023, 31(19): 30227-30238.
[13]Mulvad H C H, Abokhamis Mousavi S, Zuba V, et al. Kilowattaverage-power single-mode laser light transmission over kilometrescale hollow-core fiber[J]. Nature Photonics, 2022, 16: 448-453.
[14]A. Zhong et al., "Connecting Hollow-Core and Standard Single-Mode Fibers With Perfect Mode-Field Size Adaptation," in Journal of Lightwave Technology, vol. 42, no. 6, pp. 2124-2130, 15 March15, 2024
[15]Yu, R., Wang, C., Benabid, F., Chiang, K.S., & Xiao, L. (2021). Robust Mode Matching between Structurally Dissimilar Optical Fiber Waveguides. ACS Photonics.
[16]Zhu X Y, Wu D K, Wang Y Z, et al. Delivery of CW laser power up to 300 Watts at 1080 nm by an uncooled low-loss anti-resonant hollow-core fiber[J]. Optics Express, 2021, 29(2): 1492-1501
[17]C. Wang, J. Zhu, R. Yu, Z. Zhai and L. Xiao, "Ultralow-loss Fusion Splicing between Antiresonant Hollow-core Fibers," 2022 Asia Communications and Photonics Conference (ACP), Shenzhen, China, 2022, pp. 343-345

[18]D. Suslov,, M. Komanec, and R. Slavík, "Low loss and broadband low back-reflection interconnection between a hollow-core and standard single-mode fiber," Opt. Express 30, 37006-37014 (2022).

[19]C. Zhang et al., "Angle-Spliced SMF to Hollow Core Fiber Connection with Optimized Back-Reflection and Insertion Loss," in Journal of Lightwave Technology, vol. 40, no. 19, pp. 6474-6479, 1 Oct.1, 2022

[20]D. Suslov, D. Dousek, S. Zvanovec, E. N. Fokoua, F. Poletti, D. J. Richardson, M. Komanec, and R. Slavik, “Angled interconnection between standard single-mode fiber and nested nodeless antiresonant fibers,” in 2021 Conference on Lasers and Electro-Optics (CLEO), San Jose, CA, USA, 2021, paper Stu1Q.5

[21]Yablon, A. D. Optical Fiber Fusion Splicing; Springer: Germany, 2005.

[22]Aghaie, K. Z.; Digonnet, M. J.; Fan, S. Optimization of the splice loss between photonic-bandgap fibers and conventional singlemode fibers. Opt. Lett. 2010, 35, 1938−1940.

[23]Kakarantzas, G.; Sempere, L. P.; Russell, P. S. J. Up-tapering of optical fibers using a conventional flame tapering rig. 2007 Conference on Lasers and Electro-Optics (CLEO), May 6−11, 2007, Baltimore, MD, U.S.A., OSA: Baltimore, MD, U.S.A., 2007; pp 1−2.

[24]Love, J.; Henry, W.; Stewart, W.; Black, R.; Lacroix, S.; Gonthier, F. Tapered single-mode fibers and devices. Part 1: Adiabaticity criteria. IEE Proc.-J: Optoelectron. 1991, 138, 343−354

[25]X. Zhang, Z. Peng, Z. Dong, et al., “High-Power Mid-Infrared 2.8-μm Ultrafast Raman Laser Based on Methane-Filled Anti-Resonant Fiber,” IEEE Photonics Technol. Lett. 34(19), 1007–1010 (2022).

[26]J. P. Wooler, S. R. Sandoghchi, D. Gray, F. Poletti, M. N. Petrovich, N. V. Wheeler, N. Baddela, and D. J. Richardson, "Overcoming the Challenges of Splicing Dissimilar Diameter Solid-Core and Hollow-Core Photonic Band Gap Fibers," in Workshop on Specialty Optical Fibers and their Applications, (Optica Publishing Group, 2013), paper W3.26.